Time resolved spectroelectrochemistry studies for protection of heritage metals

A. Adriaens*[1] and M. Dowsett[2]

This paper discusses the evaluation of metal conservation treatments using a specialised electrochemical cell. The cell can be deployed in a synchrotron beam line to make *in situ*, time resolved, measurements on heritage metal alloys undergoing processes based on immersion in aqueous treatment solutions, electrochemical treatments/measurements. The present paper focuses on two specific projects: the evaluation of corrosion potential data as a simple monitoring method during the stabilisation of cupreous objects recovered from marine environments and the development and testing of a coating to protect lead objects which is stable, reversible (i.e. easy to apply and to remove), protective against corrosion and aesthetically justified.

Keywords: Cultural heritage, Metal corrosion, Spectroelectrochemistry, X-ray diffraction, X-ray absorption, Electrochemical impedance spectroscopy, Corrosion potential measurements

Introduction

Corrosion is a major problem in the degradation of heritage metal objects and any remedial measures are subject to a strong (Western) ethic which favours conservation as opposed to restoration. Besides being of fundamental interest, the study of corrosion is essential to the development of adequate conservation and preservation processes. These present major scientific challenges in the development of appropriate treatment methods for stabilisation and protection of artefacts after they are recovered from an archaeological site, and both before and during their display or storage in a museum. As inappropriate treatments can cause irreversible damage to irreplaceable objects, it is crucial that the chemical processes involved are fully understood and characterised before any preservation work is undertaken.

Until recently, conservation and preservation methods have been evaluated using *ex situ* techniques, including X-ray flourescence, X-ray diffraction (XRD), secondary electron microscopy, secondary ion mass spectrometry, etc.[1–5] This implies that the subject surface needs to be transferred from its electrolyte and/or potential environment, and placed in air or vacuum. The procedure is likely to change the surface chemistry, and precludes the real time study of the reaction.

Over the past few years, the authors have developed and tested equipment and methods for time resolved *in situ* monitoring of corrosion, passivation and coating using synchrotron X-rays and electrochemistry. The core development is an electrochemical cell (eCell) which can be used for electrochemistry (both analysis as well as treatment) with simultaneous analysis of the metal surface through a thin electrolyte layer using a spectroscopic technique (spectroelectrochemistry).[6] In contrast to other cell developments,[7–17] which as rule have concentrated on surfaces that are ideal in some way, this cell is intended for use with rough, heterogeneous metal surfaces, of either simulated alloys or fragments of real artefacts.

Recent observations from two ongoing projects are discussed in the following section. The first project deals with the simultaneous monitoring of the surface and electrochemical behaviour of archaeological copper based alloys during their storage and stabilisation. This study examines whether corrosion potential measurements E_{corr} can provide information on the effectiveness of the stabilisation and storage treatments, including the risk of repitting of artefacts by chlorine species. The second focusses on the optimisation of a protective coating for lead objects. The latter has potential for protecting organ pipes and lead objects in museum display cabinets from degradation, for example. In both projects the authors work with simulant material.

Experimental

Electrochemical cell is a specialised electrochemical cell compatible with synchrotron radiation X-ray based methods. The cell is made from Polychlorotrifluoroethylene (PCTFE) for good chemical resistance and reasonable mechanical stability. It is a cylinder 60 mm in diameter and 100 mm in height containing a piston which is driven along the bore by a stepper motor through a dynamic seal. The working electrode, whose surface forms the sample for X-ray analysis, is mounted on the piston. It can be moved precisely to translate the reacting surface from an 'electrochemical' position, in proximity to a reference electrode, through an annular platinum counter electrode to an X-ray analysis position

[1]Department of Analytical Chemistry, Ghent University, Krijgslaan 281 S12, B 9000 Ghent, Belgium
[2]Department of Physics, University of Warwick, Coventry CV4 7AL, UK

*Corresponding author, email annemie.adriaens@ugent.be

Published by Maney on behalf of the Institute
Received 19 November 2007; accepted 27 December 2007
DOI 10.1179/174329408X281759

close to a flexible 8 μm thick Kapton window. In the latter position, the path length for X-rays in the electrolyte is a fraction of a millimetre to reduce scattering and X-ray absorption. In order to establish permanent potential control on the electrode surface, a rigid polyethylene tetraphthalate inner window with a rectangular or elliptical hole in the middle is positioned just inside the Kapton, limiting the electrolyte thickness in a reproducible manner to 100–175 μm, depending on its thickness. In this way, the cell can be used down to X-ray energies below 8 keV. The two windows are tightly fastened onto the cell body by an O ring. The cell is equipped with a silver/silver chloride reference electrode and a platinum counter electrode. Figure 1 shows a cut-away diagram of the cell. The prototype of the cell used is described in more detail elsewhere.[6] The system is complimented by a webcam which allows video or stills of the eCell operation to be observed and captured.

Circular copper coupons, 12 mm in diameter (ADVENT, purity 99·9%), were made into electrodes that fit the electrochemical cell described above (see working electrode assembly in Fig. 1). The same was performed for lead (Goodfellow, purity 99·95%). The electrodes were ground on 1200 grit SiC paper to obtain a fresh surface. In the case of lead the final surface preparation consisted of abrasive polishing using 1200 grit SiC paper, rinsing with laboratory grade propan-2-ol, and wiping with a soft lint free wipe. Because the lead is so soft, the latter process provides a final burnish to the surface. For copper further smoothing of the surface was carried out using a polishing cloth covered with alumina powder of 1 μm particle size. The adherent Al_2O_3 particles on the surface were removed by immersing the samples in an ultrasonic bath containing propan-2-ol for 15 min and rinsing them thoroughly with deionised water. In addition the copper samples were corroded artificially to obtain different chloride containing corrosion products, including nantokite (CuCl) and atacamite ($Cu_2(OH)_3Cl$). Details on these corrosion protocols can be found in previous papers by Leyssens *et al.*[18,19]

X-ray absorption spectroscopy (XAS) experiments were performed at DUBBLE (station BM26A, European Synchrotron Radiation Facility, Grenoble). Cu K edge (8·979 keV) XAS spectra were recorded as a function of energy defined by the stepping of an Si (1 1 1) double crystal monochromator. The scan time was 20 min. Measurements were made in fluorescent mode using the X-ray beam at 80° to the sample surface with a nine channel monolithic Ge fluorescence detector (E&G Ortec Inc.) at 90° to the beam in order to minimise the collected flux of backscattered X-rays. This set-up results in enhanced surface specificity and a path length in the fluid of ~0·8 mm, but sample roughness can increase this. The electrochemical cell was mounted so that the sample surface was in a vertical plane.

Experiments of XRD were carried out at XMaS (station BM28, European Synchrotron Radiation Facility, Grenoble). XMaS is equipped with a Mar CCD 165 camera (Mar USA) which was used to collect the X-ray images. The time resolution (repetition rate) available is limited by the read-out time of the camera/data system to ~12 s, and typical image capture times for the authors' work lie in the range 1–60 s, so the parameters are well matched to the evaluation of processes taking minutes to days. The beamline features an 11 axis Huber goniometer with a large central ring so that the mounting of eCell or artifacts with dimensions of up to a few centimetres is straightforward. X-ray diffraction was carried out using an 8 keV beam of $\sim 10^{12}$ photons per second in multibunch mode. The beam was incident at 10° to the surface (to give the optimum compromise between path length in the fluid and surface specificity), and had a footprint of 6×1 mm. The axis of the Mar camera was placed at 35° to the beam with the camera objective plane at 130 mm from the diffraction centre. This gives a useful 2θ range of about 10 to 65° degrees and places the most significant lines across the centre of the field of view. In other experiments the authors used camera angles of 40 and 45° to extend the range of 2θ somewhat. Under these conditions, the diffraction cones are projected on the camera plane as eccentric ellipses. No available software could deal with this configuration, so the authors wrote a comprehensive image and spectrum batch processing package, esaProject (Mark Dowsett 2006, 2007) which can transform (reproject) the images into a space where the rings are straight lines for easy display and spectrum extraction.

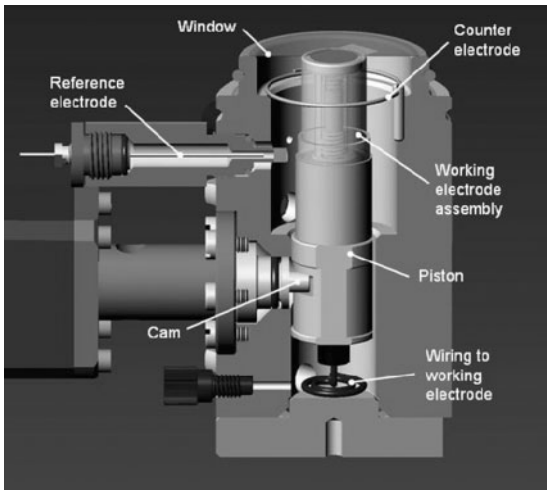

1 Schematic of electrochemical cell used in present work

Electrochemical impedance spectroscopy (EIS) data were obtained with an Autolab PGSTAT20 (Eco Chemie BV) controlled using the manufacturer's software FRA. A frequency range of 0·1 to 1000 Hz was used.

Separately, mass gain measurements were made *ex situ* using the same sodium decanoate solution.

Results

Monitoring corrosion of cupreous artefacts

It is well known that cupreous artefacts recovered from marine environments are jeopardised by exposure to air until the chlorides have been removed from the metal.[20] This is usually accomplished by soaking in tap water or dilute sodium sesquicarbonate, for a period of up to several years. Nevertheless, the metals often show some instability, such as the chemical transformation of the natural patina and the development of active corrosion.[21,22] As a result, continuous monitoring of the system remains essential. Usually this is performed by

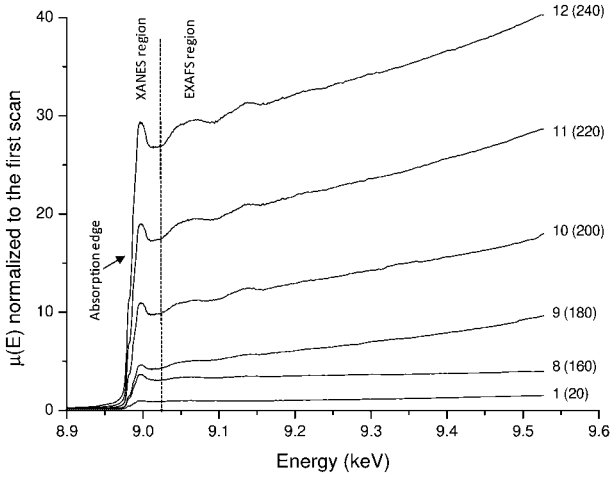

2 Sequential XAS spectra of copper/atacamite sample in sodium sesquicarbonate solution: scan numbers are indicated on right; figure in brackets is elapsed time in minutes at end of scan

measuring the chloride level at regular time intervals in the solution. The latter, however, is an indirect method in the sense that it does not provide information on the actual changes on the metal surface. Corrosion potential measurements, on the other hand, are potentially able to provide information on the surface chemistry. One hypothesis might be that, if the corrosion potential does not change as a function of time, the surface composition should be stable. A change of the corrosion potential, on the other hand, could indicate a transformation of the natural patina or the development of active corrosion.

In previous experiments this method has been evaluated using *in situ* synchrotron radiation XRD.[19] By taking simultaneous XRD and corrosion potential data on corroded copper electrodes immersed in a 1% sodium sesquicarbonate solution, the authors were able to observe the replacement of nantokite (CuCl) with the more benign cuprite (Cu_2O) in real time. It was also shown that corrosion potential measurements do not necessarily provide useful information on the effectiveness of the stabilisation and storage treatments: while the E_{corr} data seem to stabilise after 30 min of immersion, the XRD data show that nantokite continues to decrease for at least 120 min.

In order to study the continuing processes in further detail, it was decided to perform XAS measurements. The latter provide an independent means of surface characterisation as the technique is not only sensitive to the presence and evolution of amorphous surface compounds but will also give information on the presence of potential complex ions in the solution. As with the XRD experiments, eCell was filled with a 1% sodium sesquicarbonate solution (0·05 M $NaHCO_3.Na_2CO_3$) and XAS data were taken as a function of time.

The XAS spectra of the corroded copper samples, collected during their immersion in the sesquicarbonate solution, all show increasing signals as a function of time. The increase is observed both at the absorption Cu K edge, and in a proportional increase in X-ray Absorption Near Edge Structure (XANES) and Extended X-ray Absorption Fine Structure (EXAFS) modulation, but the shapes of the spectra do not appear to evolve

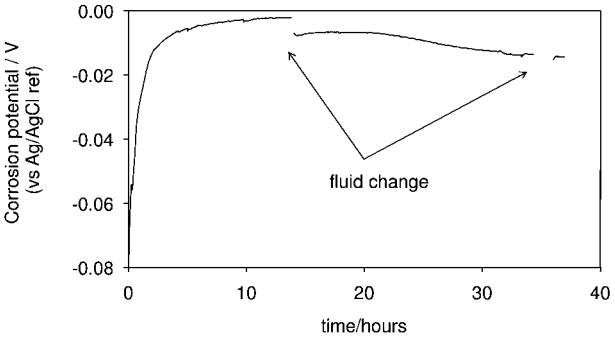

3 Corrosion potential data of copper/atacamite sample in sodium sesquicarbonate solution

strongly, even though the chemical composition of the surface is undoubtedly changing. The effect is largest for the atacamite layer, as described in what follows. Figure 2 shows the successive XAS spectra recorded for this sample. The copper edge of the first measurement is set to be equal to one. All subsequent scans are normalised to the edge height of the first scan. Scan no. 8 already shows an increase of four times with respect to the copper edge of the first measurement. From the ninth spectrum on, the increase between the different spectra becomes rapidly larger: the copper edge of spectrum 12 is $\sim$30 times as high while the EXAFS modulation has increased significantly in amplitude as well. One underlying effect, which is a continuous increase in the height of the copper edge, results in continuously increasing background slopes in the EXAFS region. The modulation in the EXAFS region also evolves slightly: from the picture presented in Fig. 2, to one which is extremely similar to the dry corrosion layer (not shown). The obvious change in the XANES or EXAFS intensity of the immersed samples could not be observed for the original dry corrosion layers, observed over similar times in air (i.e. there is no increase in signal over time for dry samples).

Figure 3 shows the corrosion potential data as a function of time. The results demonstrate that over a time period of 240 min (4 h) the corrosion potential keeps on changing, implying a continuous change of the surface chemistry. The signal stabilises after $\sim$8 h at which moment the XAS signal is still increasing (not shown).

While the spectra are being recorded and any electrochemistry is in progress, eCell makes a continuous visual record of the process using a webcam. Figure 4 shows an example of a webcam image recorded after the sample had been immersed for 30 min. The sequence of the webcam images shows the detachment of the atacamite layer from the copper substrate (not shown). A stream of atacamite drifts downwards as the sample surface is in a vertical plane on DUBBLE. Two sorts of detaching material are clearly visible: relatively large crystalline fragments up to 100 μm in size, and a 'smokelike' blue haze streaming downwards under gravity. The sudden increase in signal as of scan no. 9 can in this context be explained by the fact that at this stage more of the atacamite layer gets detached. It should be noticed, however, that the spectrum remains characteristic of atacamite throughout this process.

A possible hypothesis to cover this behaviour would be the efflorescence of small crystalline fragments from

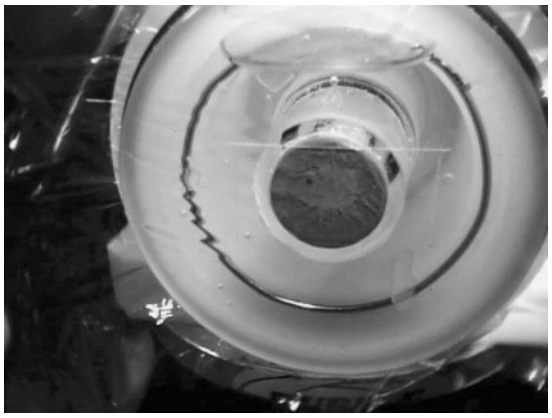

4 Webcam image of copper/atacamite surface in electrochemical cell while in solution (after 30 min immersion)

the surface into the fluid – some of these perhaps of colloidal size and supported by Brownian motion. This is further supported by the observation of a slow initial increase in the spectral intensity followed by much more rapid increases, as if the larger solid debris from the surface which have fallen to the bottom of the cell break down into large numbers of smaller particles which would be rapidly transported throughout the cell by Brownian motion. This is exactly what would happen if the crystalline material itself consists of agglomerates of small microcrystals, or had an extensive network of internal grain boundaries which were attacked by the electrolyte over time. An alternative hypothesis is that the corrosion simulation produces $CuCl_2$ mixed with the atacamite and this dissolves leaving the latter only physically connected to the surface.

Monitoring formation of protective lead coating

The combination of lead and hardwoods such as oak in close proximity is quite common. Unfortunately, the wood exudes organic acids which can attack the lead forming, for example, acetates and formates, causing serious damage, or even total loss. This problem can be exacerbated, as in the case of pipe organs, by relatively recent changes in human habits which result in warmer surroundings, large variations in relative humidity, and empty unserviced buildings. In some cases it is relatively

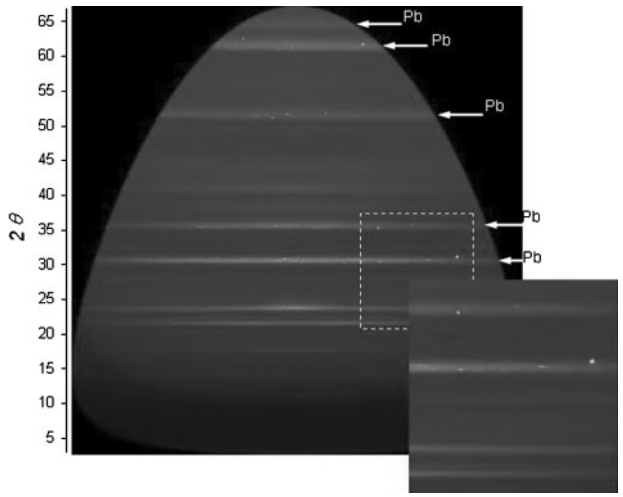

5 Reprojected X-ray diffractogramme of $Pb(C_{10})_2$ coating after 6 h growth: unlabelled lines are due to carboxylate

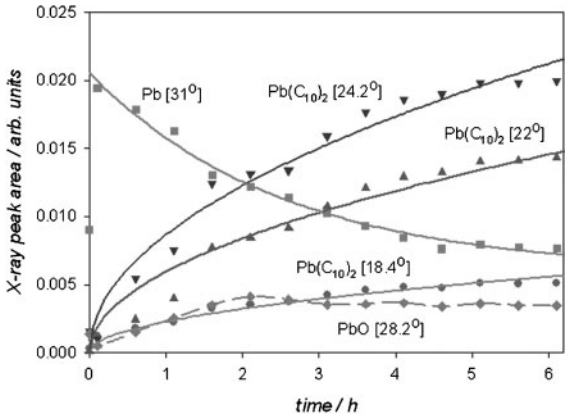

6 Time dependence of peak areas extracted from sequence of images like that in Fig. 5

simple to seek out and remove the source of the problem (e.g. the display or storage cabinet). In others the source may be furniture or technology (e.g. the wind chest of an organ) which forms an intrinsic part of the display or artefact. In such cases, one might seek an aesthetically and ethically acceptable protective coating for the lead component.

Following the work of Rocca and co-workers,[23,24] there has been considerable interest in the corrosion inhibition of the lead carboxylate coating $(CH_3(CH_2)_8COO)_2Pb$ (otherwise $Pb(C_{10})_2$ for short). In this work the authors have followed the growth of the coating in real time using synchrotron XRD in parallel with electrochemical impedance spectroscopy. For this purpose eCell was filled with ~35 mL 0·05M sodium decanoate solution. The latter was produced by neutralising 43·068 g of 99% decanoic acid (Fluka) with 0·1M 98% pure NaOH (VEL) and diluting with deionised water to a volume of 5 L. Figure 5 shows a typical reprojected X-ray image from the carboxylate coating. The arrowed features are due to the lead substrate. All the others come from the coating. The inset shows a detail of both lead and carboxylate rings. The lead ring contains spots and streaks indicative of preferred orientations in the polycrystalline surface. Conversely, all the features associated with the coating are free from internal structure showing that there is no tendency to epitaxy, and that the coating consists of small randomly oriented crystallites. This type of information is only available from an image as opposed to a 1D diffraction spectrum.

Figure 6 shows the behaviour of key peaks in the spectra extracted from the time sequence of images of which Fig. 5 is the last. The images cover a period of 6 h at intervals of 30 min. Reprojected images were integrated to spectra, normalised to the monitor count, and selected peak areas were tabulated automatically using esaProject. The data are (deliberately) not corrected for X-ray absorption in the growing layer. The peaks were selected to reflect four types of behaviour observed in the 35 or so peaks in the spectrum.

The lead area A_{Pb} shows a decrease which is well described by

$$A_{Pb} = A_0 - ae^{-bt}$$

where A_0, a and b are fitting parameters and t is time. This is approximately what one would expect from

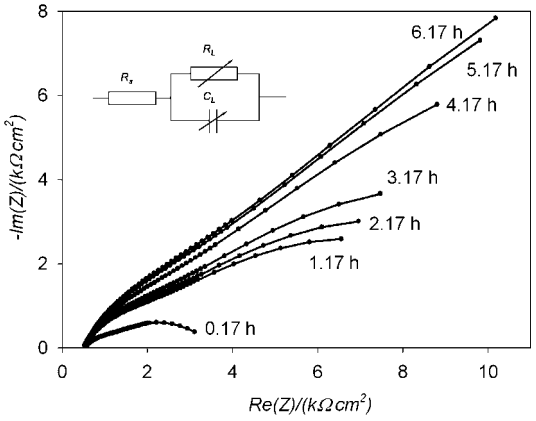

7 Nyquist plot of EIS data measured simultaneously with XRD sequence: inset shows effective model with variable impedances

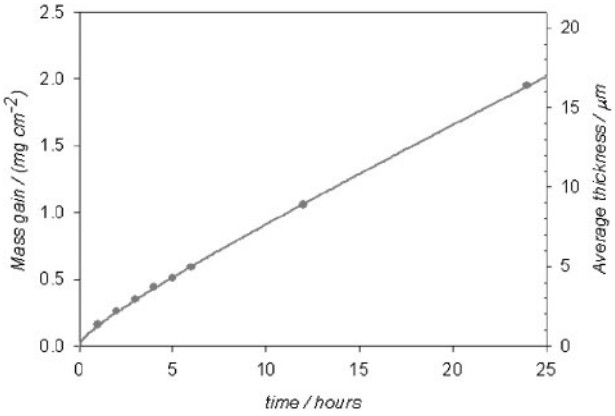

9 Mass gain and thickness data for solution used in Figs. 5 and 7

absorption of the lead orders in the growing carboxylate layer. The carboxylate peaks are fitted by parabolas

$$A_{\mathrm{Pb(C_{10})_2}} = At^{1/2}$$

In the case of the peak at 18·4°, used by Rocca *et al.*[10,11] as one of the structurally determining peaks for the carboxylate planes the parabolic growth is an extremely good fit, except towards the end where self-absorption in the layer starts to be significant (and the X-ray peak area tends to a constant value). For the other carboxylate peaks selected at 22 and 24·2°, one might argue for an initially linear behaviour in the first 4 h. One peak out of 35 observed in the spectrum, that at 28·2°, shows a completely different trend – a linear increase in the first 2 h, followed by a slight decrease in the next four. This peak is tentatively identified as the largest diffraction from PbO. This seems to grow in parallel with the carboxylate initially, and then stops as the lead becomes fully covered.

The EIS data measured simultaneously at intervals of 1 h, starting 10 min after the growth commenced are shown in the Nyquist plot of Fig. 7. The data were recorded with frequency scanned from high to low, so time runs from left to right across the plot. Because the layer grows appreciably in the time taken to make the EIS measurement (10 min), the layer capacitance and resistance must be seen as variable (inset model circuit).

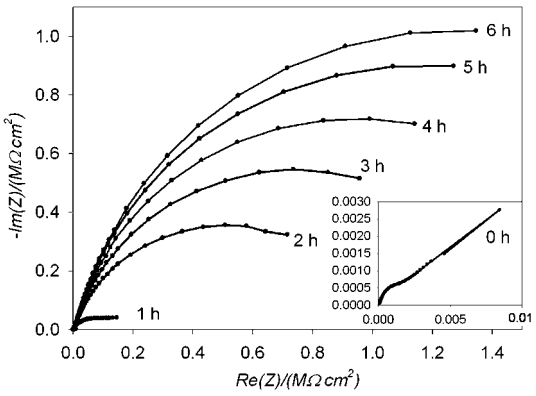

8 Data of EIS measured *ex situ* after growth in solution neutralised using more sophisticated protocol: mass gain data (points) and parabolic + linear fit (solid line) for coating deposited as in Figs. 5–7

Rather than the expected half circles, one sees, especially at the low frequencies to the right of the graph, points which are members of different half circles of progressively increasing radius. Nevertheless, one can estimate that the layer resistance is ~20 kΩ cm^2 after 6 h, rather low for a protective coating. Figure 8 shows EIS data measured ex-situ using a differently prepared sodium decanoate solution where conductivity was used as the measure of solution quality rather than pH (publication in preparation). In this case, although one must still remember that the model values are changing, the growth rate is 3–4 times lower than in the authors' simultaneous measurement and half circles are observed. The effect of growth during measurement is to stretch the half circles along the real axis and distort them slightly, making the centres appear to be more depressed than they are to the modelling programme. If a constant phase element with admittance Y_0 such that

$$Z = \frac{1}{Y_0(j\omega)^{\mathrm{n}}}$$

is used in place of C_{L}, values of n and C_{L} recovered from a fitting programme will be inaccurate. The authors are currently working on a simple dynamic model to improve this situation. However, the layer resistances are much higher ~2·6 MΩ cm^2, indicating much improved coverage of the lead. The solution used in the corrosion resistance experiments (below) was of this type.

Figure 9 shows mass gain and thickness data for the solution used in Figs. 5 and 7. Average layer thickness is calculated using a density of 1·89 g cm^{-3} (and may be slightly underestimated). The data show and initially more rapid growth rate, in good agreement with both the XRD and EIS data. The mass cm^{-2} m is well fitted by behaviour of the type

$$m = 0{\cdot}625t + 0{\cdot}091t^{1/2}$$

(a combination of linear and parabolic) which probably reflects an initial 2D crystallite spread across the surface followed by 1D vertical growth with decreased lead availability once the surface is covered. A combination of the parabolic dependence and X-ray absorption explains the approximately parabolic increase observed in the X-ray peak areas in the 6 h of the measurement in Fig. 6.

Conclusions

Making use of spectrelectrochemical measurements, it is shown that the corrosion potential does not track the surface chloride coverage: it only 'sees' the chlorides (in particular atacamite) when they are chemically attached to the substrate and not when they are physically attached. The latter can be misleading when it comes to conservation issues as chlorides may be retained in the surface and then give rise to post-treatment reactions.

It is also shown that time resolved XRD can be used to study the details of the growth of $Pb(C_{10})_2$ coatings on lead, with simultaneous electrochemical characterisation during growth. Together, the measurements suggest that two dimensional growth takes place initially, followed by one dimensional (vertical) growth when total coverage is achieved.

Acknowledgements

The authors gratefully acknowledge the following for their help: D. Richards, P. van Hoe, A. Lovejoy (cell construction); L. Bouchenoire and S. Nikitenko (beamline scientists), K. Leyssens, B. Schotte, G. Jones (help with the measurements); C. Degrigny, E. Pantos and E. Temmerman (advice and discussions). M. G. D. would like to thank Cameca GmbH for their financial support. eCell was developed using private funds from EVA Surface Analysis (UK). The work was supported by Ghent University (BOF grants) and would not have been possible without COST Action G8.

References

1. D. Guay, J. Stewart-Ornstein, X. Zhang and A. P. Hitchcock: *Anal. Chem*., 2005, **77**, 3479–3487.
2. N. Lacoudre, T. Beldjoudi and J. Dugot: in 'Metal 98', (ed. W. Mourey and L. Robbiola), 265; 1998, London, James and James.
3. M. Dowsett, A. Adriaens, M. Soares, H. Wouters, V. V. Palitsin, R. Gibbons and R. J. H. Morris: *Nucl. Instrum. Methods B*, 2005, **239B**, 51–64.
4. L. Salvo, P. Cloetens, E. Maire, S. Zabler, J. J. Blandin, J. Y. Buffiere, W. Ludwig, E. Boller, D. Bellet and C. Josserond: *Nucl. Instrum. Methods B*, 2003, **200B**, 273–286.
5. S. R. Stock: *Int. Mater. Rev*., 1999, **44**, (4), 141–164.
6. M. Dowsett and A. Adriaens: *Anal. Chem*., 2006, **78**, (10), 3360–3365.
7. M. Fleischmann, P. J. Hendra and J. Robinson: *Nature*, 1980, **288**, 152–154.
8. M. Fleischmann, A. Oliver and J. Robinson: *Electrochim. Acta*, 1986, **31**, 899–906.
9. G. G. Long, J. Kruger, D. R. Black and M. J. Kuriyama: *Electrochem. Soc*., 1983, **130**, 240–242.
10. M. Kerkar, J. Robinson and A. J. Forty: *Faraday Discus. Chem. Soc*., 1990, **89**, 31–40.
11. P. Schmuki, S. Virtanen, H. S. Isaacs, M. P. Ryan, A. J. Davenport, H. Böhni and T. J. Stenberg: *Electrochem. Soc.*, 1998, **145**, 791–801.
12. Z. Nagy and H. You: *Electrochim. Acta*, 2002, **47**, 3037–3055.
13. C. A. Lucas: *Electrochim. Acta*, 2002, **47**, 3065–3074.
14. D. Hecht, P. Borthen and H. H. Strehblow: *J. Electrochem. Soc.*, 1995, **381**, 113–121.
15. A. J. Davenport, L. J. Oblonsky, M. P. Ryan, M. F. Toney: *J. Electrochem. Soc.*, 2000, **147**, 2162–2173.
16. F. Brossard, V. H. Etgens and A. Tadjeddine: *Nucl. Instrum. Methods B*, 1997, **129B**, 419–422.
17. J. Zegenhagen, A. Kazimirov, G. Scherb, D. M. Kolb, D.-M. Smilgies and R. Feidenhans'l: *Surf. Sci.*, 1996, **352–354**, 346–351.
18. K. Leyssens, A. Adriaens, C. Degrigny, E. Pantos: *Anal. Chem*., 2006, **78**, (8), 2794–2801.
19. K. Leyssens, A. Adriaens, M. Dowsett, B. Schotte, I. Oloff, E. Pantos, A. Bell and S. Thompson: *Electrochem. Commun*., 2005, **7**, 1265–1270.
20. D. L. Hamilton: 'Methods of conserving underwater archaeological material culture', Conservation Files: ANTH 605, 'Conservation of cultural resources I', Nautical Archaeology Program, Texas A&M University, 1998, available at: http://nautarch.tamu.edu/class/ANTH605 (last visited July 2006).
21. C. V. Horie and J. A. Vint: *Studies Conserv*., 1982, 27, 185–186.
22. A. M. Pollard, R. G. Thomas and P. A. Williams: *Studies Conserv*., 1990, **35**, 148–152.
23. E. Rocca and J. Steinmetz: *Corros. Sci*., 2001, **43**, 891–902.
24. E. Rocca, C. Rapin and F. Mirambet: *Corros. Sci*., 2004, **46**, 543–665.